Evaluation of the Current Sharing Temperature of the ITER Toroidal Field Model Coil

R. Heller, D. Ciazynski, J. L. Duchateau, V. Marchese, L. Savoldi-Richard, and R. Zanino

***Abstract*—The construction and testing of the Toroidal Field Model Coil (TFMC) is part of one of the ITER large R&D projects. The main goal was to demonstrate the feasibility and the mechanical integrity of the design. One of the highlights of the first test phase was to measure the current sharing temperature, T_{CS}, of the conductor by heating the helium entering from the inlet. Because neither temperature sensors nor voltage taps are positioned inside the coil, only the helium inlet temperature and the voltage along the whole conductor length can be used for the evaluation of T_{CS}. In addition, an inner pancake joint is located at the inlet in a rather high magnetic field and the peak field region is only about 1.5 m apart from the joint. The determination of the T_{CS} relies on the exact knowledge of the thermohydraulics of both the joint and the conductor region. The paper describes and compares the different numerical models used for the evaluation of the T_{CS}. Nine T_{CS} tests at different coil currents were performed, all ending in a quench. The measured T_{CS} is in good agreement with the expectations.**

***Index Terms*—Current sharing, fusion magnets, superconductors.**

I. Introduction

THE TFMC is part of the L2 large task R&D activities [1], which are taking place in the frame of the International Thermonuclear Experimental Reactor (ITER). The TFMC was designed and constructed in collaboration between EU industries (the so-called AGAN consortium) and laboratories, coordinated by the European Fusion Development Activities (EFDA) [2], and tested in the TOSKA facility of the Forschungszentrum Karlsruhe [3]. In the first test phase, which took place during the summer and fall of 2001, the coil was tested in its self-field (peak value $\sim$7.8 T), while in a second phase, which should take place in the second half of this year, it will be tested under the additional field provided by the LCT coil (peak value $\sim$9 T).

The main goal of the TFMC program was to demonstrate for ITER the feasibility and the mechanical integrity of the design. The determination of the operation limits by evaluating the current sharing temperature of the conductor has been a substantial aim of the test program.

Magnets made with Cable-in-Conduit-Conductors (CICC), allow, in contrary to the conventional bath cooled magnets, to explore the margins by slowly increasing the temperature at constant current of the magnet up to the take-off regime. In this regime, the so-called current sharing temperature (T_{CS}) is reached by definition when the electrical field somewhere along the conductor reaches 10 μV/m. Then it is possible to compare this T_{CS} to the one given by the available model. In case of the TFMC, this was done for one of the ten pancakes.

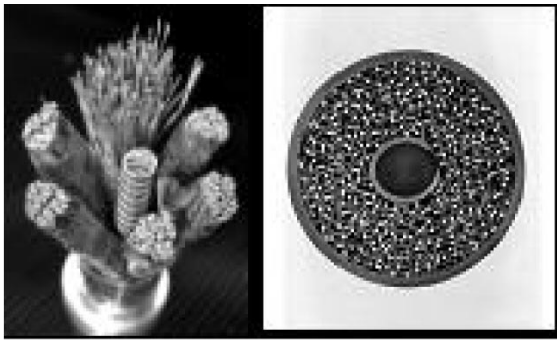

Fig. 1. Exploded (left) and cross sectional view (right) of the TFMC cable-in-conduit conductor.

It was clear from the beginning that this experiment was a challenge due to the stringent boundary conditions, under which the experiment has to be performed (proximity of the joint region from the high field region, where the current distribution is very nonuniform).

However a first analysis showed that it was quite possible to quench the conductor without quenching the joint [4], thanks also to the current redistribution, which can take place even on this short distance of 1.5 meters [5].

The TFMC conductor is a Nb_3Sn CICC jacketed with stainless steel (Fig. 1). No experience exists for such a CICC. The TF system of ITER will be made of 80 km of such a conductor. These results are therefore of essential importance for the project.

II. Exploration of TFMC Limits

The test program of Phase I included a number of items, starting from the achievement of the nominal operating current $I_{op} = 80$ kA, which was reached for the first time on July 25, 2001 [6], [7]. Here, we concentrate on the measurement of T_{CS} at different transport currents I.

According to theory, the calculation of the expected T_{CS} is not a big difficulty and should be easily performed according to the following formula when the electrical field along the CICC is 10 μV/m:

$$I_{op} = S_{noncu} J_C(B, T_{CS}, \varepsilon) \quad (1)$$

Manuscript received August 4, 2002. This work has been performed within the frame of the European Fusion Technology Programme.

R. Heller and V. Marchese are with the Forschungszentrum Karlsruhe, Institut für Technische Physik, D-76021 Karlsruhe, Germany (e-mail: reinhard.heller@itp.fzk.de).

D. Ciazynski and J. L. Duchateau are with CEA Cadarache, St. Paul lez Durance, France (e-mail: ciazyn@drfc.cad.cea.fr).

L. Savoldi-Richard and R. Zanino are with Divertimento di Energetica, Politecnico, Torino, Italy (e-mail: zanino@polito.it).

Digital Object Identifier 10.1109/TASC.2003.812736

where I_{op} is the operating current, S_{noncu} the noncopper cross section of the CICC, and J_C the critical current density as function of magnetic field (B), T_{CS} and strain (ε).

In practice, difficulties have to be pointed out in this evaluation, which is now essential for all the inserts and model coils tested in the framework of the ITER program.

A. Critical Current Density Law $J_C(B, T, \varepsilon)$

The well-known Summers law [8] is used in this case and fitted by coefficients within the quality assurance process of the fabrication of the magnets [5], where all the billets were tested at 12 T and 4.2 K and, in addition, one representative strand sample was tested at variable field and temperature [9].

On the other hand, the TFMC current sharing temperature tests have been performed at field levels from 5 to 7 T and temperatures from 8.5 to 11 K. Within these ranges of temperatures and fields, only a few data for the basic strand are available.

At such high temperatures, strand measurements are difficult to perform and temperature uniformity is very difficult to reach. In addition, measurements were performed on a titanium barrel mandrel and the strain is around -0.2%, which is also rather different from the strain in a steel jacketed CICC.

This situation is a source of uncertainty, which has to be mentioned.

B. Consideration on the Strain ε

Both the critical current density of Nb_3Sn and the current sharing temperature are very sensitive to longitudinal strain. In the TFMC, during the heat treatment of the conductor performed at about 650 °C, due to the differential thermal compression between the conductor jacket and the strand, the filaments are put in compression loading to a high value of the so-called thermal strain. No direct measurement has ever been performed on any full size conductor; the exact strain of the Nb_3Sn filament in such a conductor is therefore unknown. The only set of data available comes from a mechanical experiment performed on sub-size (36 strands) conductors with different kinds of jackets [10].

The conclusion which can be drawn from that experiment, is that the bonded model is appropriate to describe the situation. In this model, it is supposed that there is no sliding between the jacket and the conductor during heat treatment.

Although the strain is classically considered in this kind of experiment as a fitting parameter deduced from the data, the expected strain according to the bonded model should be in the range of about -0.7%.

The total strain in the Nb_3Sn filaments is $\varepsilon = \varepsilon_o + \varepsilon_{op}$, where ε_o is the strain at zero current and ε_{op} is the applied strain due to coil deformation under electromagnetic load. $\varepsilon_{op} = \varepsilon_{op}(x)$. The strain ε_{op} which varies along the conductor length is derived from FEM computation [11], its maximum value is reached at peak field location and is $+0.072\%$ at 80 kA. ε_o may be composed of $\varepsilon_{ht} + \varepsilon_{\mathrm{deg}}$ where $\varepsilon_{ht} = -0.61\%$ comes from the relaxed fully-bonded model, and $\varepsilon_{\mathrm{deg}}$ denotes an additional compression (or degradation).

C. Magnetic Field B

Due to the self-field of the conductor, which is not negligible in case of the TFMC, each strand travels through the cable section within one cable twist, experiencing at 80 kA a field from 7.24 T on the inner side of the conductor to 5.9 T on the outer side. The difference in T_{CS} corresponding to these two magnetic fields is in the order of 0.5 K.

Practically, the corresponding T_{CS} can be calculated by integrating the electrical field over the CICC cross section.

$$E = E_C/S \int (J_{op}/J_C(B, T, \varepsilon))^n \, dS, \tag{2}$$

where E_c is the critical electrical field (equal to 10 μV/m), S the cable cross section, and n is the so-called n value.

D. Consideration on the n Value and Current Distribution

The calculation presented so far depends on the n value. Little attention has been paid up to now to this parameter in the specific conditions of strain, field and temperature as in the TFMC. The n value is decreasing with the critical current and the limit explorations are performed at low critical current [12]. Exploring the TFMC limit at 80 kA, this corresponds to strand critical current of 111 A. Unfortunately, the TFMC take-off characteristic will be of little help to identify this n value due to the proximity of the joint to the high field point. In the joint region, the current distribution is highly nonuniform. So, this take-off characteristic is strongly influenced by the redistribution process, taking place between the joint and the high field point (about 1.5 m) and cannot give information about the strand n value.

III. Description of Experiment and Results

Details on the experimental set-up are given in [13], so only a brief overview will be given. After current ramping and plateau, the helium entering the DP1.2 pancake (at the inner joint) was slowly heated up to the quench. Note that the neighboring pancake in the same radial plate (and connected to the same inner joint) DP1.1 was also heated to approximately the same level in order to limit the thermal exchange between both. The voltage drop over the whole DP1.2 pancake was measured using co-wound voltage taps. Nine quench experiments were performed, but among them only a few are really usable and trustable because of measuring accuracy problems encountered on these low level voltage signals.

Fig. 2 shows the measured voltage drop U along DP1.2 as a function of the inlet temperature T_{in} for three runs at 80 kA and one run for 56.6 kA. Using (2) and expressing J_C as a function of the critical temperature T_C, one gets

$$U/U_C = ((T^* - T)/(T^* - T_C))^{-n}, \tag{3}$$

where T^* is a free parameter but has to be not much larger than T_{CS} because of the linear approach used.

From the fits, it is possible to derive the n value but not T_{CS}. To deduce the grade of a (possible) degradation of the TFMC conductor, a more physical model is needed. In the following,

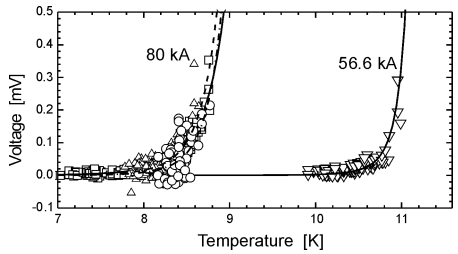

Fig. 2. Voltage along pancake DP1.2 versus inlet temperature for different conductor currents of the TFMC.

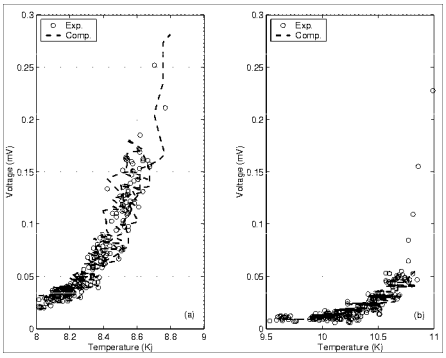

Fig. 3. Comparison of voltage-temperature characteristics at (a) 80 kA and at (b) 56.6 kA. Symbols represent experimental data, dashed lines are best-fits computed by M&M.

we have used both the last 80 kA and 56.6 kA experiments because they look really usable.

IV. Analysis Using the M&M Code

Details of the M&M analysis are given in [14] and only a short overview will be given here. The main emphasis of using a thermohydraulic model of the TFMC was to compute the temperature profile along the conductor starting from the heater, which is at the inlet of DP1.1 and DP1.2, modeling the DP1 inner joint and ending in the conductor.

The knowledge of the actual helium temperature at the location of the initial normal zone in relation to the temperature at the heater outlet is essential for the exploration of T_{CS}, since no temperature sensor is located within the winding. With the multi-step heating procedure developed using M&M, the whole scenario was simulated. The thermohydraulic analysis showed that the difference between the inlet temperature and T_{CS} is within $\pm$0.2 K.

The M&M code has been modified to be able to model the actual operational strain ε_{op} in the conductor. Then, the "actual" critical parameters (n, ε) are obtained from the best-fit of U–T_{in} curves [using the experimental $T_{in}(t)$ as boundary condition]. The result is shown in Fig. 3, where the experimental and the computed characteristics are compared. The best fits correspond to $n = 7$, $\varepsilon_0 = -0.75\%$ at 80 kA, and $n = 4$–5, $\varepsilon_0 = -(0.64$–$0.67)\%$ at 56.6 kA.

From this analysis it may be concluded that a degradation with respect to the measured strand properties has to be added to explain the TFMC conductor behavior as a collection of strands carrying a uniform current at the average field. This

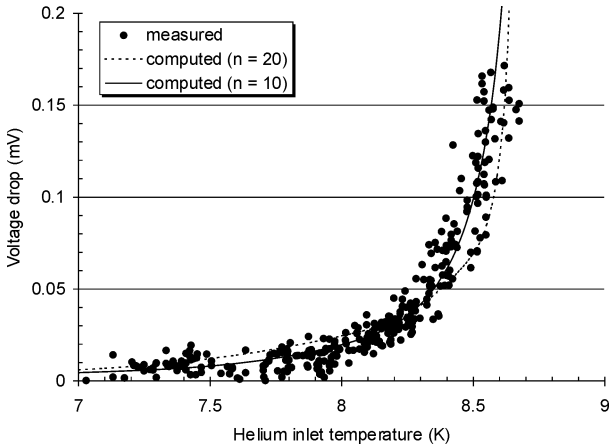

Fig. 4. Voltage drop versus inlet temperature at 80 kA (ENSIC/exp.).

TABLE I
Units for Magnetic Properties

Current [kA]	56.6 kA			80.0 kA		
n_{strand}	20	15	10	20	15	10
ρ_t ($\mu\Omega$.m)	100	70	30	100	60	25
ε_o (%)	-0.63	-0.64	-0.65	-0.69	-0.71	-0.73

strand degradation increases with operating current, but only two data points are available, so further work is needed on this point in phase II of the TFMC tests. The TFMC cable appears to be characterized by n values (4–7) much smaller than those of the strand (15–20), and decreasing for decreasing current (i.e., increasing temperature).

V. Electrical Analysis Using the ENSIC Code

The electrical network model ENSIC has been developed at CEA to represent the whole DP1.2 pancake. This network model includes a realistic modeling of the joints, leading to an uneven current distribution among the strands of the cable, but not among the petals [15]. The magnetic field gradient across the conductor, as well as the angle between field and strand (twisted cable) are taken into account [15]. This model has been validated using experimental results on full size conductor samples [16]. The ENSIC code now includes a simplified steady state thermohydraulic model, calculating the profile along the conductor length from the inlet temperature, taking into account the Joule heating in the joints and in the regular conductor. The heat exchanges with the adjacent pancake as well as in the joint are neglected.

There are only 3 free parameters in the model: the strand n value n_{strand}, the interstrand resistivity in the conductor ρ_{t_cond} [15], and ε_o. These parameters have been adjusted to best fit the experimental voltage drop measured across the DP1.2 pancake (excluding the joints) as function of the inlet temperature, at 56.6 kA and 80 kA (see Fig. 4). The results are given in Table I.

It can be seen in Table I and Fig. 4 that similar results can be obtained using different (n_{strand}-ρ_t-ε_o) combinations. Indeed, a cable low n value n_{cable} can be obtained either by a more uniform current distribution and a lower n_{strand}, or by a less uniform current distribution and a higher n_{strand}.

TABLE II
MAIN RESULTS OF THE T_{CS} ANALYSIS OF THE TFMC

Current [kA]	Model	T_{loc} (K)	ε_0 [%][(b)]	n_{cable}
56.6	M&M	10.87 [(a)] – 10.90 [(b)]	-(0.64 – 0.67)	4 - 5
	ENSIC	10.83 ± 0.1	-(0.64±0.01)	N/A
	Expectation	10.68		
80	M&M	8.33 [(a)] – 8.41 [(b)]	-0.75	7
	ENSIC	8.43 ± 0.1	-(0.71±0.02)	N/A
	Expectation	8.47		

[(a)] cable at 10 μV/m, [(b)] $\varepsilon_0 = \varepsilon_{ht} + \varepsilon_{deg.}$, N/A = not available

A value of 15–20 for n_{strand} should be expected. However, the lowest values of ρ_t seem more realistic with respect to the results obtained on the full size samples [16], which should lead to $n_{strand} = 10$. The real value of n_{strand} is therefore hard to derive from experimental results due to the proximity of the peak field to the inner joint.

Finally, it can be said that: $\varepsilon_o = -0.64\% \pm 0.01\%$ at 56.6 kA, and: $\varepsilon_o = -0.71\% \pm 0.02\%$ at 80 kA. Note that the (absolute) values of ε_o are higher than expected (-0.61%) [5], and that ε_o should not depend on the coil current, therefore an increase of $|\varepsilon_0|$ is the signature of a degradation as current increases. The origin of this degradation is not yet clear, but it could well be due to a real increase of the strain as the internal electromagnetic force increases. A possible explanation is given in [17].

The ENSIC code can compute at peak field both the local average electric field in the cable and the local temperature, which are not directly measurable. The local temperature at an electric field of 10 μV/m, which is called the cable T_{CS}, can be compared to the expected T_{CS} from strand properties, calculated with the expected $\varepsilon_o = -0.61\%$ (see Table II) [5].

T_{CS} is then only slightly below the expectation at 80 kA, and is even above at 56.6 kA. From this point of view, the conductor performances look as expected from strand properties. This result is however quite surprising since we use degraded strand performances (see ε_o), and moreover the current distribution is not uniform among strands. Such a result comes in fact from the high magnetic field gradient across the cable section ($\Delta B/B = \pm 10\%$), indeed T_{CS} has been calculated, as usually, at the maximum field in the section, while the ENSIC code is taking into account the field gradient.

VI. COMPARISON OF ANALYSIS RESULTS

The different results are compared to each other. In Table II, the different results are compared to each other. It turned out that T_{CS} is quite similar at 10 μV/m criterion for both models but the total strain is different especially at 80 kA.

All the values calculated by ENSIC used the low field correction of J_C, which is equivalent to only $+0.02\%$ on ε_o. Other differences between ENSIC and M&M lie also in the nonuniform current distribution (ENSIC), the heat exchange (M&M), and the choice of "best" fits.

In Fig. 5, the T_{CS} is plotted as a function of the current. It reflects that the results are delimited by the expected values on one side and by the strand properties using the average magnetic field on the other side.

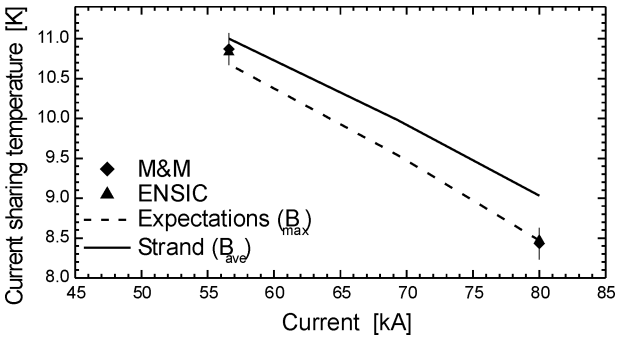

Fig. 5. Current sharing temperature versus current: expectations, experimental, and analysis results.

VII. CONCLUSION AND CONSIDERATIONS FOR ITER DESIGN

The quench experiments performed on the TFMC were a first very interesting opportunity to explore the limits of large stainless steel jacketed CICC such as the one which is needed for the TF system of ITER. Different tools like the M&M and ENSIC codes were developed and appear to be suitable for detailed studies on these systems.

The TFMC performance is in agreement with the expectations and demonstrated the capacity of such conductors for ITER. However, a refined analysis showed that there is a degradation of strand performances which is larger at larger $I \times B$. The apparent "good" coil performances are due to the high field gradient across the cable.

Since the TFMC operated at low magnetic field, an error bar on J_C is paid by a significant error on ε [10% on J_C results in 0.05% (absolute) on ε]. So one needs a better characterization of the strand under TFMC operating conditions, and to confirm these results in Phase II operation.

The predictions for the ITER TF coil require a significant extrapolation in $I \times B$ (max. realized in TFMC is so far 525 kN/m, while 775 kN/m is expected in the ITER TF). From the present knowledge, the extrapolations should lead to about -0.80% for $\varepsilon_{ht} + \varepsilon_{\mathrm{deg}}$, which is quite high. However, this extrapolation has to be taken with caution taking into account all the error bars and the only 2 available data points.

REFERENCES

[1] T. Mizoguchi and N. Mitchell, "ITER R&D: Magnets: Introduction," *Fusion Engineering and Design*, vol. 55, pp. 139–140, 2001; N. Mitchell, E. Salpietro "ITER R&D: Magnets: Toroidal Field Model Coil," *Fusion Engineering and Design*, vol. 55, pp. 171–190, 2001.

[2] E. Salpietro, "A toroidal field model coil for the ITER-FEAT project," *IEEE Trans. Appl. Supercond.*, vol. 12, pp. 623–628, 2002.

[3] P. Komarek and E. Salpietro, "The test facility for the ITER TF model coil," *Fusion Engineering and Design*, vol. 41, pp. 213–221, 1998.

[4] L. Savoldi and R. Zanino, "Predictive study of current sharing temperature test in the toroidal field model coil without LCT coil using the M&M code," *Cryogenics*, vol. 40, pp. 539–548, 2000.

[5] J. L. Duchateau *et al.*, "Electromagnetic evaluation of the collective behavior of 720 twisted strands for the TFMC," *IEEE Trans. on Appl. Supercond.*, vol. 11, p. 1538, 2001.

[6] H. Fillunger *et al.*, "Assembly in the test facility, acceptance and first test results of the ITER TF model coil," *IEEE Trans. Appl. Supercond.*, vol. 12, pp. 595–599, 2002.

[7] J. L. Duchateau *et al.*, "Test program preparations of the ITER TFMC," *Fusion Engineering and Design*, vol. 58–59, pp. 147–151, 2001.

[8] L. T. Summers *et al.*, "A model for the prediction of Nb3Sn critical current as a function of field, temperature, strain and radiation damage," *IEEE Trans. Mag.*, vol. 27, pp. 2041–2044, 1991.
[9] A. Martinez and J. L. Duchateau, "Field and temperature dependencies of critical current on industrial Nb3Sn strands," *Cryogenics*, vol. 37, p. 865, 1997.
[10] W. Specking, J. L. Duchateau, and P. Decool, "First results of strain effects on critical current of incoloy jacketed Nb3Sn CIC 'S'," in *Proc. 15th Int. Conf. on Magnet Technology*. Beijing, 1998.
[11] S. Raff, "Stress analysis for the TFMC tests in TOSKA: Conductor strain in pancake P1," *Internal Note IRS 04/02, Fusion*, vol. 187, May 2002.
[12] R. Maix, private communication.
[13] L. Savoldi *et al.*, "First measurement of the current sharing temperature at 80 kA in the ITER Toroidal Field Model Coil (TFMC)," *IEEE Trans. Appl. Supercond.*, vol. 12, pp. 635–638, 2002.
[14] R. Zanino and L. Savoldi, "Measurement of the current sharing temperature and performance evaluation of the ITER Toroidal Field Model Coil," *Cryogenics*, 2002, submitted for publication.
[15] T. Schild, D. Ciazynski, and S. Court, "Effect of actual cabling pattern on the critical current of a multistage CIC," *Adv. in Cryo. Eng.*, vol. 46B, p. 1051, 2000.
[16] D. Ciazynski and J. L. Duchateau, "Validation of the CEA electrical network model for the ITER coils," *IEEE Trans. on Appl. Supercond.*, vol. 11, p. 1530, 2001.
[17] N. Mitchell, "Analysis of the effect of Nb3Sn strand bending on CICC superconductor performance," *Cryogenics*, vol. 42/5, pp. 311–325, 2002.